Zone-based Physics-Informed Neural Network (Z-PINN) for Addressing Data Scarcity in Ceramic Sintering Processes

Seungwan Woo
Department of Artificial Intelligence
University of Science and Technology
Deajeon, Republic of Korea
seungwan@etri.re.kr

Abstract— Recent advances in artificial intelligence have enabled predictive modeling and control in manufacturing processes. However, industrial datasets often suffer from missing entries and limited availability due to sensor limitations, failures, and high installation costs. Physics-Informed Neural Networks (PINNs) incorporate physical laws into the learning process, offering physically consistent predictions, but their performance deteriorates in complex processes when relying on a single global partial differential equation (PDE) or ordinary differential equation (ODE). To address this limitation, we propose a Zone-based PINN (Z-PINN) framework that divides the process timeline into multiple zones based on a predefined ceramic sintering schedule and trains a separate PINN for each zone. Without modifying the original PINN structure, this approach allows localized learning and improves prediction accuracy while ensuring physical consistency. We evaluate Z-PINN on real ceramic sintering data under three scenarios: short-term missing values, long-term missing values, and full sequence generation from minimal initial inputs. Experimental results show that Z-PINN significantly outperforms the conventional PINN in all cases, achieving lower Root Mean

Keywords—PINN, Physics-Informed Learning, Industrial AI, Manufacturing, Ceramic sintering process

Squared Error (RMSE) and Mean Absolute Error (MAE), and

producing physically consistent outputs even in data-scarce

I. INTRODUCTION

Artificial intelligence (AI)-based technologies have been actively adopted in the manufacturing industry for process automation, quality prediction, and anomaly detection [1,2]. The aging workforce and retirement of experienced operators have led to increasing reliance on unskilled personnel, exposing the limitations of human-centered control and decision-making in processes requiring high precision [3]. The concept of the smart factory has emerged to address this challenge, demanding high-precision control systems capable of replacing the tacit knowledge of skilled workers [4].

The core of smart factories lies in models that predict and control quality and process conditions using data collected from equipment and sensors, which play a vital role in maintaining consistent quality [5]. Industrial environments often face limitations in data acquisition due to inaccessible equipment, costly inspection tools, and high sensor installation expenses [6]. Also, missing data—both long-term and short-term—frequently occur as a result of equipment failures or sensor malfunctions [7]. Such data losses reduce the reliability of model training and may significantly compromise process stability and product quality if the system state at missing timestamps cannot be reconstructed [8,9].

The quantity of data available per process unit is generally limited in manufacturing settings. Industrial AI applications

* Corresponding author

Hyunwoo Oh*

ICT-enabled Intelligent Manufacturing Research Section

Electronics and Telecommunications Research Institute

Deajeon, Republic of Korea

hyunwoo@etri.re.kr

frequently suffer from data scarcity, especially when compared to approaches trained on large-scale public datasets [10,11]. Interpolating missing values, estimating unobserved data points, and generating reliable training datasets from limited observations becomes essential [12,13].

To address these challenges, this study proposes a datadriven learning approach guided by physical laws. A Physics-Informed Neural Network (PINN) framework [14] is adopted, embedding physical equations into the loss function to ensure physical consistency during training. PINNs have demonstrated effectiveness in both predictive accuracy and interpretability across various physical domains, including heat transfer, fluid dynamics, and structural mechanics [15,16,17].

Conventional PINNs utilize global partial differential equation (PDE) or ordinary differential equation (ODE)-based loss formulations, which often lead to degraded performance in complex systems characterized by abrupt process condition changes or highly nonlinear dynamics [18,19]. This paper introduces a Zone-based PINN (Z-PINN) framework to overcome this limitation. The process is divided into time-based zones according to the sintering schedule, and each zone is independently modeled using a separate PINN. The effectiveness of the proposed method is experimentally validated using real power and temperature data collected from a ceramic sintering process, with results compared against conventional PINN models.

II. BACKGROUND AND MOTIVATION

The ceramic sintering process plays a crucial role in determining final product quality, including key properties such as density, mechanical strength, and color [21]. Electric furnaces utilize supplied power as a primary control variable that directly influences the internal temperature of the furnace, thereby impacting the overall quality of the ceramics. Power consumption is closely linked to energy usage, constituting a critical factor in achieving energy-efficient process control [22].

Accurate acquisition of power and temperature data is essential for both quality prediction and optimal control in ceramic manufacturing. Missing values frequently arise due to sensor aging or failure, which can impair control precision and degrade the performance of predictive models. Reliable reconstruction of missing data is necessary to mitigate these effects [8,9].

Conventional deep learning-based interpolation methods estimate missing values by identifying patterns within the data. These methods do not incorporate physical constraints, causing the resulting outputs to potentially violate fundamental physical principles, leading to unreliable predictions and physically inconsistent synthetic data [13].

The Physics-Informed Neural Network (PINN) framework addresses this issue by integrating physical laws into the learning process through a composite loss function comprising Physics Loss, Initial Condition Loss (IC Loss), and Boundary Condition Loss (BC Loss), thereby enforcing compliance with predefined physical relationships [15,16,17].

Traditional PINNs are trained using a single global partial differential equation (PDE) or ordinary differential equation (ODE), which limits their applicability in processes exhibiting abrupt transitions or heterogeneous zone-specific characteristics. This performance degradation stems from attempting to model complex localized dynamics using a single governing equation [18,19,20].

To overcome this limitation, we propose a novel Zone-based PINN (Z-PINN) framework. In our approach, process data are segmented into time-based zones, and each zone is independently modeled and trained. This allows for finer representation of localized behaviors, resulting in enhanced interpolation accuracy and improved adherence to physical consistency.

III. PROPOSED METHOD

This section introduces the proposed Zone-based Physics-Informed Neural Network (Z-PINN) framework, which trains individual PINN models for each time-based zone to capture complex process dynamics.

Ceramic sintering typically follows a predefined tem Ceramic sintering typically follows a predefined temperature schedule over time, where phases such as heating, soaking, and cooling occur sequentially. Each phase exhibits different power and temperature change patterns. Modeling the entire process using a single physical law cannot effectively represent these nonlinear and complex dynamics.

Power serves as a response variable regulated by the controller to achieve the target temperature, and it exhibits nonlinear variation depending on process conditions and external factors. In contrast, the sintering process is designed based on a target temperature schedule, as shown in Table I. Therefore, dividing the process into zones based on time is justified and reflects physical meaning.

TABLE I. CERAMIC SINTERING SCHEDULE

Time (T)	Target (° C)	Time (T)	Target (° C)
$0.00 \le T \le 2.00$	~ 100	$27:00 \le T \le 28:00$	600
2:00 ≤ T < 3:00	100	28:00 ≤ T < 36:00	~1200
3:00 ≤ T < 18:00	~400	36:00 ≤ T < 36:20	1200
18:00 ≤ T < 19:00	400	$36:20 \le T \le 48:20$	~1635
19:00 ≤ T < 27:00	~600	48:20 ≤ T < 51:50	1635

The process is divided into multiple zones based on the temperature schedule, as illustrated in Fig. 1, enabling the capture of locally consistent behaviors within each zone. The overall Z-PINN architecture is presented in Fig. 2. Each zone is trained independently using a PINN that shares the same network structure, the same embedded physical laws (Physics Loss), and the same components—Initial Condition Loss (IC Loss) and Boundary Condition Loss (BC Loss). This modular design allows for flexible application without modifying the underlying PINN architecture.

In the actual dataset, the full sintering process is divided into 10 zones, as shown in Table I. An optimal approximating function is trained for each zone and subsequently concatenated to form a continuous time-series prediction.

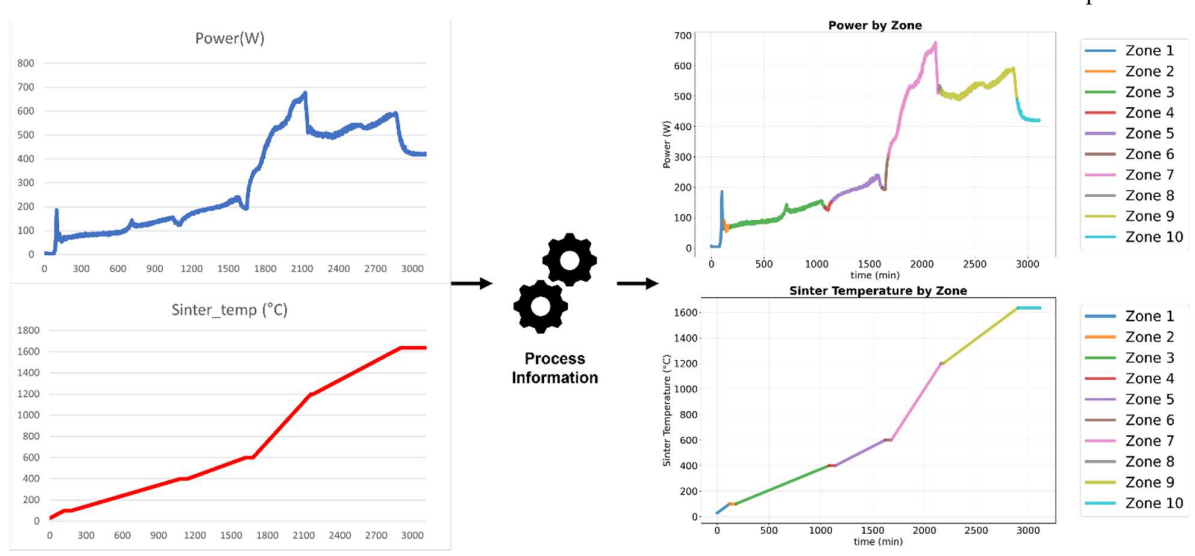


Fig. 1. Time-based segmentation of the ceramic sintering process according to the temperature schedule.

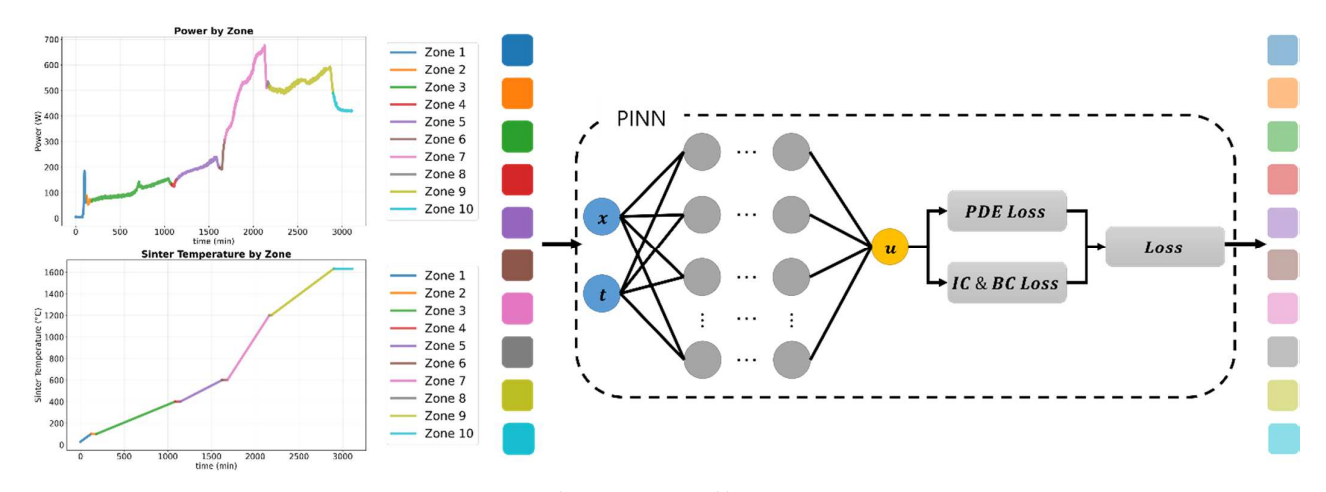


Fig. 2. Z-PINN Architecture

IV. EXPERIMENTS

This section outlines the dataset, training configuration, and experimental results. The performance of the proposed Z-PINN framework is compared with that of a conventional PINN under three scenarios: short-term missing value interpolation, long-term missing value interpolation, and data generation. Root Mean Squared Error (RMSE) and Mean Absolute Error (MAE) are used as evaluation metrics.

$$RMSE = \sqrt{\frac{1}{n} \sum_{i=1}^{n} (y_i - \hat{y})^2}$$
 (1)

$$MAE = \frac{1}{n} \sum_{i=1}^{n} |y_i - \hat{y}_i|$$
 (2)

A. Dataset

Eight real-world ceramic sintering cycles were utilized. Of these, five cycles were used for training, two for validation, and one for testing, as summarized in Table II. Each cycle contains 3,110 minutes of data sampled at one-minute intervals. The dataset includes power, furnace temperature, ambient temperature, humidity, and pressure, as detailed in Table III.

TABLE II. SPLIT OF CERAMIC SINTERING DATA

Train	Validation	Test	Total
5 Cycle	2 Cycle	1 Cycle	8 Cycle

TABLE III. EXAMPLE OF SINTERING CYCLE DATASET STRUCTURE

Cycle_ID	Time_min	Power (W)	Sinter_temp (°C)
1	0	5.39513	15.7
1	1	3.940303	16.4025
i	:	:	:
1	3110	427.7182	1635
Env_temp	Atmospheric pressure(hPa)		Humidity (%)
15.7	1000.8		65
15.7	1000.8		66
÷	:		:
23.9	1008.1		42

The primary prediction targets are furnace temperature and power. Representative patterns of the data are illustrated in Fig. 3. Three types of missing data scenarios were simulated as follows:

- 1) Short-term Missing (MCAR): Randomly removed 30% of the test data to simulate sensor noise and short-term faults.
- 2) Long-term Missing: Removed all data except every 15-minute sample to simulate sustained sensor failure.
- 3) Data Generation: Provided only initial values and required the model to generate the full time-series under given physical laws.

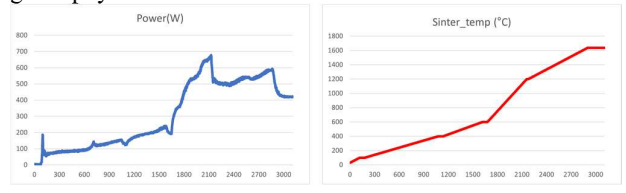


Fig. 3. Target data patterns (Left: Power(W), Right: Sinter temp(°C))

B. Short-term Missing Interpolation

The results for short-term missing interpolation are presented in Fig. 4, Fig. 5, and Table VI. The Z-PINN framework outperformed the conventional PINN across all evaluation metrics. For temperature prediction, RMSE was reduced from 36.6611 to 2.8904, and MAE from 15.7514 to 0.8619. For power prediction, RMSE decreased from 18.0662 to 11.0881, and MAE from 5.5840 to 4.0831.

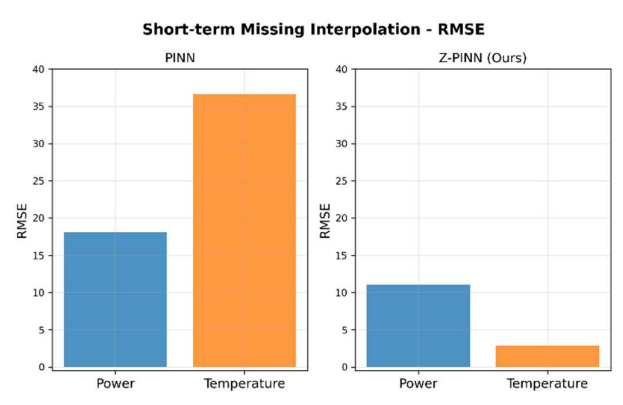


Fig. 4. Performance of short-term missing value interpolation (RMSE)

Short-term Missing Interpolation - MAE

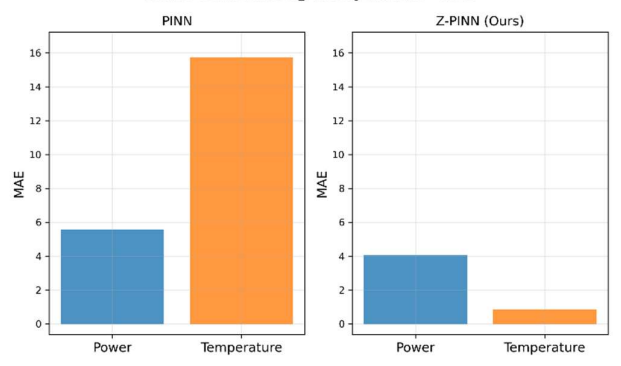


Fig. 5. Performance of short-term missing value interpolation (MAE)

TABLE IV. RESULTS FOR SHORT-TERM MISSING VALUE INTERPOLATION

	RMSE		MAE	
	Power	Temperature	Power	Temperature
PINN	18.0662	36.6611	5.5840	15.7514
Z-PINN (ours)	11.0881	2.8904	4.0831	0.8619

C. Long-term Missing Interpolation

The results for long-term missing data are shown in Fig. 6, Fig. 7, and Table V. Z-PINN achieved substantial performance improvements. For temperature, RMSE was reduced from 65.8009 to 5.1061, and MAE from 49.5570 to 2.6361. For power, RMSE decreased from 62.4661 to 22.9087, and MAE from 41.6128 to 13.4768.

Long-term Missing Interpolation - RMSE

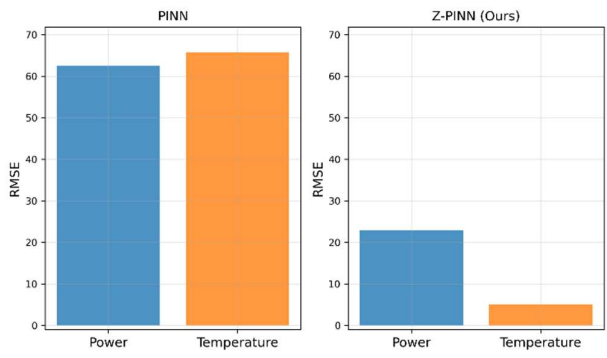


Fig. 6. Performance of long-term missing value interpolation (RMSE)

Long-term Missing Interpolation - MAE

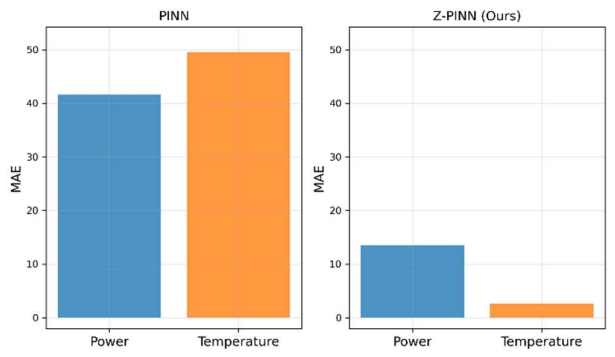


Fig. 7. Performance of long-term missing value interpolation (MAE)

TABLE V. RESULTS FOR LONG-TERM MISSING VALUE INTERPOLATION

	RMSE		MAE	
	Power	Temperature	Power	Temperature
PINN	62.4661	65.8009	41.6128	49.5570
Z-PINN (ours)	22.9087	5.1061	13.4768	2.6361

D. Data Generation

In the data generation scenario, Z-PINN was tasked with predicting the full time-series from initial values alone. As illustrated in Fig. 8, Fig. 9, and Table VI, Z-PINN demonstrated significant improvements. For temperature, RMSE decreased from 68.1179 to 5.2983, and MAE from 53.0980 to 2.8306. For power, RMSE fell from 64.6231 to 23.7596, and MAE from 44.5730 to 14.4779. The generated trends, visualized in Fig. 10 and Fig. 11, closely followed the actual physical behavior of the process.

Data Generation - RMSE

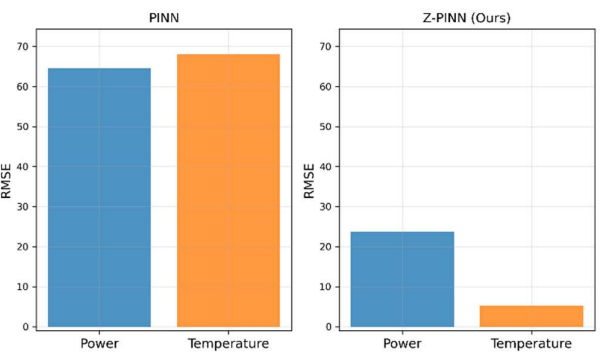


Fig. 8. Performance of Data Generation (RMSE)

PINN Z-PINN (Ours) 50 40 40 20 10 10 Power Temperature Power Temperature

Fig. 9. Performance of Data Generation (MAE)

TABLE VI. RESULTS FOR DATA GENERATION

	RMSE		MAE	
	Power	Temperature	Power	Temperature
PINN	64.6231	68.1179	44.5730	53.0980
Z-PINN (ours)	23.7596	5.2983	14.4779	2.8306

E. Complexity, Latency, and Memory

We evaluate computational complexity, latency, and memory of the proposed Z-PINN against a conventional PINN from both algorithmic and empirical perspectives.

Algorithmically, a fully connected layer of shape $m \times n$ costs roughly 2mn FLOPs. Under this count, Z-PINN (5–64–32–1) requires about 4.8k FLOPs per forward pass, whereas the conventional PINN (5–128–256–128–64–32–1) requires about 153k FLOPs, a~32× gap.

Empirically, on an RTX 4060 with PyTorch 2.7.1 (eval mode, batch=1; 50 warm-ups, 200 timed iterations, measured via CUDA events), each sample is processed only by its corresponding zone-specific model (no cross-zone ensembling). Z-PINN achieves 0.098 ms (p50) / 0.119 ms (p95), while the conventional PINN requires 0.316 ms / 0.350 ms (~3.2× speed-up). Parameter counts are 24,970 vs. 78,209 (Z-PINN is ~3.1× smaller), corresponding to FP16 model sizes of 0.048 MB vs. 0.149 MB. Peak inference memory is ~0.0092 GB for both, dominated by CUDA runtime/allocator overheads given the small models.

For completeness, we also report a conservative upper-bound bulk measurement where all zone models are run sequentially on the entire test set (non-selective): 0.0072 s (average per zone model) for Z-PINN vs. 0.0174 s for the conventional model. Sequential training wall-clock on the same GPU is 21.53 s for Z-PINN (10 zones) and 84.16 s for the conventional model. (Data sizes: Z-PINN used 4,680 samples in total; the conventional model 5,000; Zone 8 had 180 samples.) Accuracy (MAE/RMSE/MSE) favors Z-PINN across scenarios.

F. Summary

Z-PINN exhibited superior performance compared to the conventional PINN across all scenarios:

- In short-term interpolation, RMSE was reduced by approximately 38.6% for power and 92.1% for temperature.
- In long-term missing scenarios, Z-PINN provided stable predictions even under severely limited observations.
- In data generation tasks, Z-PINN successfully synthesized physically consistent time-series data from minimal initial input.



Fig. 10. Power (W) predictions in the data generation scenario (Left: Ground Truth, Center: PINN, Right: Z-PINN(ours))

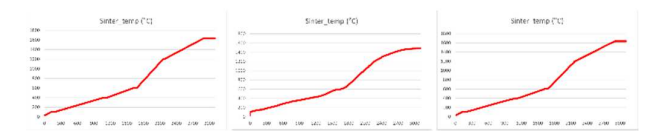


Fig. 11. Sinter_temp (°C) predictions in the data generation scenario (Left: Ground Truth, Center: PINN, Right: Z-PINN(ours))

V. CONCLUSION

This paper proposed a Zone-based PINN (Z-PINN) framework that segments the ceramic sintering process into multiple time-based zones according to the temperature schedule and derives optimal approximating functions for

each zone using independent PINNs. The approach preserves the original PINN architecture and effectively captures localized physical behaviors.

Experimental results on real sintering data demonstrated that Z-PINN outperforms conventional PINNs across short-term and long-term interpolation scenarios, as well as in data generation from minimal inputs. Both RMSE and MAE metrics were consistently lower, and the generated time-series outputs maintained strong physical consistency even under severe data scarcity.

However, localized errors still appeared in zones with highly nonlinear transitions, such as the initial heating phase. Future work will focus on improving zone segmentation strategies and integrating hybrid physical models to further enhance prediction accuracy and physical fidelity in complex industrial processes.

ACKNOWLEDGMENT

This work was supported by Korea Evaluation Institute of Industrial Technology(KEIT) grant funded by the Korea government(MOTIE)(RS-2023-00259964, Development of Auto Re-learning Common Service Platform Technology for Ceramic Industry DX based on Cloud)

REFERENCES

- R. X. Gao, J. Krüger, M. Merklein, H.-C. Möhring, and J. Váncza, "Artificial Intelligence in manufacturing: State of the art, perspectives, and future directions," *CIRP Annals*, vol. 73, no. 2, pp. 723–749, Jan. 2024
- [2] I. Elía and M. Pagola, "Anomaly detection in Smart-manufacturing era: A review," *Engineering Applications of Artificial Intelligence*, vol. 139, p. 109578, Nov. 2024.
- [3] A. W. Stedmon, H. Howells, J. R. Wilson, and I. Dianat, "Ergonomics/Human factors needs of an ageing workforce in the manufacturing sector.," *PubMed*, Jan. 2012.
- [4] E. Fenoglio, E. Kazim, H. Latapie, and A. Koshiyama, "Tacit knowledge elicitation process for industry 4.0," *Discover Artificial Intelligence*, vol. 2, no. 1, Mar. 2022.
- [5] P. Zheng et al., "Smart manufacturing systems for Industry 4.0: Conceptual framework, scenarios, and future perspectives," Frontiers of Mechanical Engineering, vol. 13, no. 2, pp. 137–150, Jan. 2018.
- [6] F. Ghafari, E. Shourangiz, and C. Wang, "Cost effectiveness of the industrial Internet of things adoption in the U.S. manufacturing SMEs," *Intelligent and Sustainable Manufacturing*, vol. 1, no. 1, p. 10008, Jan. 2024.
- [7] X. Yuan et al., "Missing Data Imputation for Industrial Time Series with Adaptive Median Iteration based on Generative Adversarial Networks," *IEEE Sensors Journal*, p. 1, Jan. 2024.
- [8] L. Ma, M. Wang, and K. Peng, "A missing manufacturing process data imputation framework for nonlinear dynamic soft sensor modeling and its application," *Expert Systems With Applications*, vol. 237, p. 121428, Sep. 2023.
- [9] P. Nunes, J. Santos, and E. Rocha, "Challenges in predictive maintenance – A review," CIRP Journal of Manufacturing Science and Technology, vol. 40, pp. 53–67, Nov. 2022.
- [10] Y. F. Zhao, J. Xie, and L. Sun, "On the data quality and imbalance in machine learning-based design and manufacturing—A systematic review," *Engineering*, Jul. 2024.
- [11] L. Alzubaidi et al., "A survey on deep learning tools dealing with data scarcity: definitions, challenges, solutions, tips, and applications," *Journal of Big Data*, vol. 10, no. 1, Apr. 2023.
- [12] H. Ekwaro-Osire, S. L. Ponugupati, A. A. Noman, D. Bode, and K.-D. Thoben, "Data augmentation for numerical data from manufacturing processes: an overview of techniques and assessment of when which techniques work," *Industrial Artificial Intelligence*, vol. 3, no. 1, Jan. 2025.
- [13] V. Buggineni, C. Chen, and J. Camelio, "Enhancing manufacturing operations with synthetic data: a systematic framework for data

- generation, accuracy, and utility," Frontiers in Manufacturing Technology, vol. 4, Feb. 2024.
- [14] M. Raissi, P. Perdikaris, and G. E. Karniadakis, "Physics-informed neural networks: A deep learning framework for solving forward and inverse problems involving nonlinear partial differential equations," *Journal of Computational Physics*, vol. 378, pp. 686–707, Nov. 2018.
- [15] Z. Zhao, Y. Wang, W. Zhang, Z. Ba, and L. Sun, "Physics-informed neural networks in heat transfer-dominated multiphysics systems: A comprehensive review," *Engineering Applications of Artificial Intelligence*, vol. 157, p. 111098, Jun. 2025.
- [16] C. Zhao, F. Zhang, W. Lou, X. Wang, and J. Yang, "A comprehensive review of advances in physics-informed neural networks and their applications in complex fluid dynamics," *Physics of Fluids*, vol. 36, no. 10. Oct. 2024.
- [17] J. Qi, K. Du, H. Luo, Z. Wang, and R. Wen, "Physics-informed neural networks for Structural Dynamic Response Analysis: theoretical and Numerical verification," *International Journal of Structural Stability* and Dynamics, Apr. 2025.

- [18] S. Wang, X. Yu, and P. Perdikaris, "When and why PINNs fail to train: A neural tangent kernel perspective," *Journal of Computational Physics*, vol. 449, p. 110768, Oct. 2021.
- [19] A. S. Krishnapriyan, A. Gholami, S. Zhe, R. M. Kirby, and M. W. Mahoney, "Characterizing possible failure modes in physics-informed neural networks," *Neural Information Processing Systems*, vol. 34, Dec. 2021.
- [20] A. Henkes, H. Wessels, and R. Mahnken, "Physics informed neural networks for continuum micromechanics," *Computer Methods in Applied Mechanics and Engineering*, vol. 393, p. 114790, Mar. 2022.
- [21] Q. Chen et al., "Machine Learning-Assisted Multi-Property prediction and sintering mechanism exploration of Mullite-Corundum Ceramics," Materials, vol. 18, no. 6, p. 1384, Mar. 2025.
- [22] J. Chen et al., "An Energy-Efficient sintering temperature multimode control and optimization for High-Quality Ternary Cathode materials," *Deleted Journal*, p. 100034, Jan. 2025.